International Journal of Modern Physics C
Vol. 28, No. 4 (2017) 1750044 (20 pages)

DOI: 10.1142/S0129183117500449

World Scientific
www.worldscientific.com

Corrections to finite-size scaling in the 3D Ising model based on nonperturbative approaches and Monte Carlo simulations

J. Kaupužs[*,†,‡,¶], R. V. N. Melnik[‡,§,‖] and J. Rimšāns[†,‡]

[*]*Institute of Technical Physics, Riga Technical University*
Laboratory of Semiconductor Physics
Paula Valdena Str. 3/7, LV-1048, Riga, Latvia

[†]*Institute of Mathematical Sciences and Information Technologies*
University of Liepaja, 14 Liela Street, Liepaja LV–3401, Latvia

[‡]*The MS2 Discovery Interdisciplinary Research Institute*
Wilfrid Laurier University, Waterloo, Ontario, Canada, N2L 3C5

[§]*BCAM - Basque Center for Applied Mathematics*
E48009 Bilbao, Spain
[¶]*kaupuzs@latnet.lv*
[‖]*rmelnik@wlu.ca*

Received 15 November 2016
Accepted 28 December 2016
Published 21 April 2017

In Memoriam: This paper is dedicated to the memory of our colleague and friend, Professor Janis Rimshans, who recently passed away. He was a wonderful person and a great scientist who is missed by many of us who had an honor and privilege to work with him.

Corrections to scaling in the 3D Ising model are studied based on nonperturbative analytical arguments and Monte Carlo (MC) simulation data for different lattice sizes L. Analytical arguments show the existence of corrections with the exponent $(\gamma-1)/\nu \approx 0.38$, the leading correction-to-scaling exponent being $\omega \leq (\gamma-1)/\nu$. A numerical estimation of ω from the susceptibility data within $40 \leq L \leq 2560$ yields $\omega = 0.21(29)$, in agreement with this statement. We reconsider the MC estimation of ω from smaller lattice sizes, $L \leq 384$, using different finite-size scaling methods, and show that these sizes are still too small, since no convergence to the same result is observed. In particular, estimates ranging from $\omega = 0.866(21)$ to $\omega = 1.247(73)$ are obtained, using MC data for thermodynamic average quantities, as well as for partition function zeros. However, a trend toward smaller ω values is observed in one of these cases in a refined estimation from extended data up to $L = 1536$. We discuss the influence of ω on the estimation of critical exponents η and ν.

Keywords: Ising model; corrections to scaling; nonperturbative methods; Feynman diagrams; critical couplings; Monte Carlo simulation.

PACS Nos.: 75.10.Hk, 64.60.an, 05.10.Ln, 64.60.Cn, 05.50.tq

[¶]Corresponding author.

1. Introduction

The critical exponents of the three-dimensional (3D) Ising universality class have been a subject of extensive analytical as well as Monte Carlo (MC) studies during many years. The results of the standard perturbative renormalization group (RG) methods are well known.[1–5] An alternative analytical approach has been proposed in Ref. 6 and further analyzed in Ref. 7, where this approach is called the Grouping of Feynman Diagrams (GFD) theory. A review of MC work till 2001 is provided in Ref. 8. More recent papers are Refs. 9–13.

In this paper, we will focus on the exponent ω, which describes the leading corrections to scaling. A particular interest in this subject is caused by recent challenging nonperturbative results reported in Ref. 14, showing that $\omega \leq (\gamma - 1)/\nu$ holds in the φ^4 model based on a rigorous proof of certain theorem. The scalar 3D φ^4 model belongs to the 3D Ising universality class with $(\gamma - 1)/\nu \approx 0.38$. Therefore, ω is expected to be essentially smaller than the values of about 0.8 predicted by standard perturbative methods and currently available MC estimations. The results in Ref. 14 are fully consistent with the predictions of the alternative theoretical approach of Ref. 6, from which $\omega = 1/8$ is expected. We have performed a MC analysis of the standard 3D Ising model, using our data for very large lattice sizes L up to $L = 2560$, to clarify whether ω, extracted from such data, can be consistent with the results of Refs. 6 and 14. Since our analysis supports this possibility, we have further addressed a related question on how a decrease in ω influences the MC estimation of critical exponents η and ν. We have also tested different finite-size scaling methods of estimating ω from smaller lattice sizes to check whether such methods always give ω consistent with 0.832(6), as one can expect from Ref. 9.

Models with the so-called improved Hamiltonians are often considered instead of the standard Ising model for a better estimation of the critical exponents.[9,10] The basic idea of this approach is to find such Hamiltonian parameters, for which the leading correction to scaling vanishes. However, this correction term has to be large enough and well detectable for the estimation of ω. So, this idea is not very useful in our case.

Our results, along with the recent studies of nonperturbative effects by other authors[15] emphasize the importance of the nonperturbative approaches in study of critical phenomena.

2. Analytical Arguments

We consider the continuous φ^4 model in the thermodynamic limit of diverging volume $V \to \infty$ with the Hamiltonian $\mathcal{H}$ given by

$$\frac{\mathcal{H}}{k_B T} = \int \left(r_0 \varphi^2(\mathbf{x}) + c(\nabla \varphi(\mathbf{x}))^2 + u\varphi^4(\mathbf{x})\right) d\mathbf{x}, \tag{1}$$

where the order parameter $\varphi(\mathbf{x})$ is an n-component vector with components $\varphi_i(\mathbf{x})$, depending on the coordinate $\mathbf{x}$, T is the temperature, and k_B is the Boltzmann constant.

As in Ref. 14, we assume that there exists the upper cut-off parameter Λ for the Fourier components of the order-parameter field $\varphi_i(\mathbf{x})$, whereas the temperature-dependence of the Hamiltonian parameters in vicinity of the critical temperature T_c is given by a linear relation

$$r_0 = r_{0c} + a(T - T_c), \tag{2}$$

where r_{0c} is the critical value of r_0 and a is a constant. The parameters c and u are assumed to be T-independent, and we consider only the case $T > T_c$ (or $r_0 > r_{0c}$).

The leading singular part of specific heat $C_V^{\rm sing}$ of this model can be expressed as[14]

$$C_V^{\rm sing} \propto \xi^{1/\nu} \left(\int_{k<\Lambda} [G(\mathbf{k}) - G^*(\mathbf{k})] d\mathbf{k} \right)^{\rm sing}, \tag{3}$$

assuming the power-law singularity $\xi \sim t^{-\nu}$ of the correlation length ξ at small reduced temperature $t \to 0$. Here, $G(\mathbf{k})$ is the Fourier-transformed two-point correlation function, and $G^*(\mathbf{k})$ is its value at the critical point.

Nonperturbative analytical calculations have been performed in Ref. 14 to evaluate the $\mathbf{k}$-space integral (3) based on certain scaling assumptions. Namely, the leading singularity of specific heat has the form of $C_V^{\rm sing} \propto (\ln \xi)^{\lambda} \xi^{\alpha/\nu}$ and the two-point correlation function has the asymptotic form of $G(\mathbf{k}) = \sum_{\ell \geq 0} \xi^{(\gamma - \theta_\ell)/\nu} g_\ell(k\xi)$, $G^*(\mathbf{k}) = \sum_{\ell \geq 0} b_\ell k^{(-\gamma + \theta_\ell)/\nu}$. In these expressions, α, γ and ν are the critical exponents of specific heat, susceptibility and correlation length, respectively. In addition, the leading term has exponent $\theta_0 = 0$, whereas the subleading terms with $\ell \geq 1$ have correction-to-scaling exponents $\theta_\ell > 0$. These expressions are consistent with the conventional scaling hypothesis, $g_\ell(k\xi)$ being the scaling functions. The exponent λ is responsible for possible logarithmic correction in specific heat, whereas the usual power-law singularity is recovered at $\lambda = 0$.

In addition to these scaling arguments, an extra assumption has been used in Ref. 14 that the contribution of small-k region $k < \Lambda'$ is relevant at $\lim_{\Lambda' \to 0} \lim_{\xi \to \infty}$. It has been verified by an MC simulation test in the lattice φ^4 model.[14]

The results of analytical calculations have been formulated as a theorem in Ref. 14, the mentioned here scaling assumptions (along with certain natural assumptions concerning the exponents and scaling functions) being formulated as conditions of the theorem. The precise formulation of the theorem is given on p. 1650108-5 of Ref. 14. Basically, this theorem implies that the two-point correlation function contains a correction-to-scaling exponent $\theta_\ell = \gamma + 1 - \alpha - d\nu$, if this expression is positive. Taking into account the well-known hyperscaling hypothesis $\alpha + d\nu = 2$, we thus have $\theta_\ell = \gamma - 1$ if $\gamma > 1$. According to the finite-size scaling theory, it implies the existence of correction-to-scaling exponent $\omega_\ell = (\gamma - 1)/\nu$ in the finite-size scaling. Moreover, ω_ℓ is not necessarily the leading correction-to-scaling exponent. Therefore, $\omega \leq (\gamma - 1)/\nu$ holds for the leading correction-to-scaling exponent ω. Thus we have $\omega_\ell = 3/4$ and $\omega \leq 3/4$ in the two-dimensional (2D) φ^4 model, where $\gamma = 7/4$ holds, as in the 2D Ising model.

As discussed in Ref. 14, nontrivial corrections tend to be canceled out in the 2D Ising model, in such a way that only trivial ones with integer θ_ℓ are usually observed.

However, there is no reason to assume such a scenario in the 3D case. The theorem of Ref. 14 refers to the 2D, as well as 3D φ^4 models. Therefore, the existence of corrections with the exponent $(\gamma-1)/\nu$ is expected in the 3D Ising model, since it belongs to the same universality class as the 3D φ^4 model. Because this correction is not necessarily the leading one, the prediction is $\omega \leq \omega_{\max}$, where $\omega_{\max} = (\gamma-1)/\nu$ is the upper bond for the leading correction-to-scaling exponent ω. Using the widely accepted estimates $\gamma \approx 1.24$ and $\nu \approx 0.63$ (Ref. 3) for the 3D Ising model, we obtain $\omega_{\max} \approx 0.38$. The prediction of the GFD theory[6] is $\gamma = 5/4$, $\nu = 2/3$ and, therefore, $\omega_{\max} = 0.375$. Thus, we can state that in any case $\omega_{\max}$ is about 0.38. The value of ω is expected to be $1/8$ according to the GFD theory considered in Refs. 6 and 7.

One of the basic aims of our MC analysis in this paper is to test these challenging predictions.

3. Monte Carlo Simulation Results

3.1. *Simulations at various pseudo-critical couplings*

3.1.1. *The general method*

We have simulated the 3D Ising model on simple cubic lattice with periodic boundary conditions. The Hamiltonian H of the model is given by

$$H/T = -\beta \sum_{\langle ij \rangle} \sigma_i \sigma_j, \tag{4}$$

where T is the temperature measured in energy units, β is the coupling constant and $\langle ij \rangle$ denotes the pairs of neighboring spins $\sigma_i = \pm 1$. The MC simulations have been performed with the Wolff single cluster algorithm,[16] using its parallel implementation described in Ref. 17. An iterative method has been used in Ref. 17 to find pseudo-critical couplings $\tilde{\beta}_c(L)$ corresponding to certain value $U = 1.6$ of the ratio $U = \langle m^4 \rangle / \langle m^2 \rangle^2$, where m is the magnetization per spin. Following this method, we have performed simulations at various pseudo-critical couplings to test several methods of estimation of the correction-to-scaling exponent ω. In particular, well-known methods[9,18] are based on the analysis of U and $U_6 = \langle m^6 \rangle / \langle m^2 \rangle^3$ (and several similar dimensionless ratios of magnetization moments) at such couplings, where these quantities scale as $A + BL^{-\omega}$ at $L \to \infty$.

Our iterative method[12,17] includes the calculation of derivatives to find a given pseudo-critical coupling and various average quantities at this coupling by using the Taylor series expansion in its vicinity. In particular, the derivative $\partial \mathcal{A}/\partial \beta$ of an arbitrary quantity $\mathcal{A}$ is calculated from

$$\frac{\partial}{\partial \beta} \langle \mathcal{A} \rangle = N[\langle \mathcal{A} \rangle \langle \varepsilon \rangle - \langle \mathcal{A} \varepsilon \rangle], \tag{5}$$

where $\varepsilon = -N^{-1} \sum_{\langle ij \rangle} \sigma_i \sigma_j$ is the mean energy per spin, $N = L^3$ being the total number of spins. Similarly, derivatives of higher orders are also calculated in terms of statistical averages, according to the Boltzmann statistics.

3.1.2. *The case of* $U = 1.6$

As in our earlier paper,[12] we have used the pseudo-critical coupling $\tilde{\beta}_c(L)$, corresponding to $U = 1.6$, to evaluate the susceptibility $\chi = L^3\langle m^2\rangle$ and the derivative $\partial Q/\partial\beta$ at $\beta = \tilde{\beta}_c(L)$, where $Q = 1/U$. The results for $16 \leq L \leq 1536$ have already been reported in Table 1 of Ref. 12. We have extended the simulations to lattice sizes $L = 1728$, $L = 2048$ and $L = 2560$, using approximately the same number of MC sweeps (spin flips per N) as for $L = 1536$ in Ref. 12. Thus, Table 1 of Ref. 12 can now be completed with the new results presented in Table 1 here.

3.1.3. *The case of specific heat maximum*

One of the possibilities is to choose the pseudo-critical coupling $\hat{\beta}_c(L)$, corresponding to the maximum of specific heat C_V. We have determined the corresponding values of U from our earlier simulation results, discussed in Ref. 13. The data for $L \leq 384$ are given in Table 2.

Table 1. The values of $\tilde{\beta}_c$, as well as χ/L^2, and $10^{-3}\partial Q/\partial\beta$ at $\beta = \tilde{\beta}_c$ depending on L.

L	$\tilde{\beta}_c$	χ/L^2	$10^{-3}\partial Q/\partial\beta$
2560	0.2216546217(52)	1.1669(28)	213.4(1.6)
2048	0.2216546252(66)	1.1741(27)	151.1(1.1)
1728	0.2216546269(94)	1.1882(20)	116.98(87)

Table 2. The pseudo-critical couplings $\hat{\beta}_c$ and the values of U at $\beta = \hat{\beta}_c$ depending on the linear system size L.

L	$\hat{\beta}_c$	U
384	0.22167526(52)	1.1884(62)
320	0.22168192(69)	1.1901(63)
256	0.22169312(76)	1.1937(50)
192	0.2217149(10)	1.1940(42)
160	0.2217347(14)	1.1951(44)
128	0.2217742(16)	1.1831(32)
96	0.2218366(24)	1.1917(33)
80	0.2219002(32)	1.1885(32)
64	0.2220057(42)	1.1888(30)
48	0.2221987(58)	1.1930(27)
40	0.2223761(76)	1.1933(26)
32	0.222659(10)	1.1983(26)
24	0.223195(12)	1.2035(19)
20	0.223686(13)	1.2051(16)
16	0.224443(15)	1.2121(13)
12	0.225813(16)	1.22147(93)
10	0.226903(18)	1.23159(86)
8	0.228567(20)	1.24474(64)

3.1.4. *The case of* $Z_a/Z_p = 0.5425$

We have applied our iterative method also in MC simulations with pseudo-critical coupling $\grave{\beta}_c(L)$, corresponding to $Z_a/Z_p = 0.5425$, as in Refs. 18 and 19. Here Z_a and Z_p are partition functions for the model with antiperiodic and periodic boundary conditions, respectively. The scaling form of U and U_6 is not influenced by the precise value of Z_a/Z_p, but $Z_a/Z_p = 0.5425$ is a known[18] approximation for the universal critical value of Z_a/Z_p at $\beta = \beta_c$ and $L \to \infty$. The simulations have been performed by the boundary flip algorithm, discussed in Refs. 19 and 20. In this algorithm, the spin system is flipped between the states with periodic and antiperiodic boundary conditions with certain probabilities. If the corresponding cluster algorithm (see Ref. 19) is implemented in such a way that there is always just one seed spin per cluster in the boundary flip step, then $Z_a/Z_p = p$ is equal to the probability p that the flip from periodic to antiperiodic state is accepted. It can be determined from simulations with periodic boundary conditions without real flipping to the antiperiodic state.[19] We have followed this method in our simulations, determining p as $p = \langle s \rangle$, where $s = 1$, if the flip is accepted, and $s = 0$ otherwise. The derivative $\partial p/\partial\beta$, required for the iterative finding of $\grave{\beta}_c(L)$, is calculated from (5).

In our simulations, MC measurements have been performed after each $L/8$ (rounding up for $L = 6$ and $L = 12$) Wolff clusters. It corresponds to ≈ 0.16 MC sweeps between successive measurements. The acceptance test of the boundary flip has been performed after each five measurements. One iteration included 125 000 measurements for $L \geq 128$ and $(128/L) \times 125\,000$ measurements for $L < 128$. Totally, 120 iterations have been used in MC estimations for every size L, discarding the first four iterations from each simulation run. Thus, the total number of MC sweeps $\mathcal{N}_{\rm sw}$, used in the estimations at a given L, is about 2.4×10^6 for $L \geq 128$ and even larger for $L < 128$.

As compared to the simulations in Ref. 17, the total number of Wolff clusters (for not discarded iterations) is increased by factor of 2 for $L \leq 128$ and by factor of 4.14 for $L = 384$ to obtain more accurate results. Correspondingly, $\mathcal{N}_{\rm sw}$ is increased by almost the same factors. The simulation results for $\grave{\beta}_c(L)$ and the corresponding values of U and U_6 within $8 \leq L \leq 384$ are given in Table 3.

Two different pseudo-random number generators, discussed and tested in Ref. 12, have been used in these and other MC simulations of this paper to verify that the results agree within error bars of about one or, sometimes, two standard deviations.

3.1.5. *The case of* $\xi_{\rm 2nd}/L = 0.6431$

We have performed MC simulations also for pseudo-critical coupling $\bar{\beta}_c(L)$, corresponding to $\xi_{\rm 2nd}/L = 0.6431$, as in Ref. 9, where 0.6431 is an approximate critical value of this ratio. Here, $\xi_{\rm 2nd}$ is the second moment correlation length $\sqrt{[(\chi/G(2\pi/L)) - 1]/[4\sin^2(\pi/L)]}$, in accordance with Refs. 8 and 14, $G(k)$ being the Fourier-transformed two-point correlation function in the $\langle 100 \rangle$ direction. As in the case of Z_a/Z_p, the precise value of $\xi_{\rm 2nd}/L$ is not important in our scaling analysis.

Table 3. The pseudo-critical couplings $\grave{\beta}_c$ and the values of U and U_6 at $\beta = \grave{\beta}_c$ depending on the linear system size L.

L	$\grave{\beta}_c$	U	U_6
384	0.221654638(11)	1.60039(76)	3.0897(23)
256	0.221654653(19)	1.59990(72)	3.0874(22)
192	0.221654721(36)	1.59980(65)	3.0867(22)
128	0.221654685(65)	1.59826(65)	3.0791(22)
96	0.221655153(94)	1.59577(55)	3.0697(20)
64	0.22165574(15)	1.59404(47)	3.0606(16)
48	0.22165703(20)	1.59102(42)	3.0457(16)
32	0.22166087(33)	1.58658(27)	3.0247(13)
24	0.22166661(43)	1.58139(24)	3.0006(13)
16	0.22168605(61)	1.57174(18)	2.9553(10)
12	0.22171844(76)	1.56297(14)	2.91393(95)
8	0.2218185(15)	1.54523(12)	2.83035(85)

The MC measurements have been performed after each $L/2$ Wolff clusters. The number of iterations, discarded iterations and MC sweeps in these simulations is similar to those for $Z_a/Z_p = 0.5425$, except only for the two largest sizes. In particular, $\mathcal{N}_{\text{sw}}$ is decreased by factor of ≈ 1.6 for $L = 1280$ and by factor of ≈ 2.4 for $L = 1536$ as compared to the almost constant value of $\mathcal{N}_{\text{sw}}$ (around 2.35×10^6) within $128 \leq L \leq 1024$. The simulation results for $\bar{\beta}_c(L)$ and the corresponding values of U and U_6 within $8 \leq L \leq 1536$ are given in Table 4.

Table 4. The pseudo-critical couplings $\bar{\beta}_c$ and the values of U and U_6 at $\beta = \bar{\beta}_c$ depending on the linear system size L.

L	$\bar{\beta}_c$	U	U_6
1536	0.2216546251(47)	1.60270(93)	3.1009(41)
1280	0.2216546194(51)	1.60165(71)	3.0966(31)
1024	0.2216546177(63)	1.60223(54)	3.0989(23)
864	0.2216546253(81)	1.60179(55)	3.0980(24)
768	0.2216546096(87)	1.60272(52)	3.1013(23)
640	0.221654632(11)	1.60312(57)	3.1023(25)
512	0.221654616(15)	1.59984(56)	3.0890(25)
432	0.221654621(20)	1.60067(56)	3.0922(25)
384	0.221654607(22)	1.60058(61)	3.0918(27)
320	0.221654699(30)	1.60216(49)	3.0980(21)
256	0.221654685(44)	1.60004(50)	3.0891(22)
216	0.221654598(58)	1.59868(52)	3.0828(23)
192	0.221654746(74)	1.59922(52)	3.0850(23)
160	0.221654927(97)	1.59885(51)	3.0835(22)
128	0.22165469(13)	1.59772(57)	3.0780(25)
108	0.22165476(15)	1.59727(45)	3.0778(27)
96	0.22165490(18)	1.59557(44)	3.0681(19)
80	0.22165539(22)	1.59550(36)	3.0672(16)

Table 4. (*Continued*)

L	$\bar{\beta}_c$	U	U_6
64	0.22165530(26)	1.59380(32)	3.0593(14)
54	0.22165642(25)	1.59211(27)	3.0513(12)
48	0.22165642(34)	1.59104(25)	3.0462(11)
40	0.22165743(41)	1.58936(26)	3.0381(11)
32	0.22166131(53)	1.58643(23)	3.02425(94)
27	0.22166437(60)	1.58377(23)	3.01220(93)
24	0.22166676(66)	1.58148(20)	3.00122(83)
20	0.22167152(83)	1.57787(20)	2.98419(84)
16	0.2216823(12)	1.57252(16)	2.95893(65)
12	0.2217109(14)	1.56377(13)	2.91737(54)
10	0.2217418(16)	1.55678(11)	2.88449(46)
8	0.2218008(22)	1.546454(96)	2.83564(39)

3.2. *Partition function zeros*

Searching for a different method, we have evaluated the Fisher zeros of partition function from MC simulations by the Wolff single cluster algorithm, following the method described in Ref. 11. The results for $4 \leq L \leq 72$ have been reported in Ref. 11. We have performed high statistics simulations with MC measurements after each $\max\{2, L/4\}$ Wolff clusters, omitting 10^6 measurements from the beginning of each simulation run, and totally 5×10^8 measurements used in the analysis for each L within $4 \leq L \leq 128$. The latter number has been reduced to 3×10^8, 2×10^8 and 1.4×10^8 for $L = 192$, $L = 256$ and $L = 384$, respectively. Considering $\beta = \eta + i\xi$ as a complex number, the results for the first Fisher zero $\mathrm{Re}\, u^{(1)} + i\, \mathrm{Im}\, u^{(1)}$ in terms of $u = \exp(-4\beta)$ are reported in Table 5. Our values are obtained, evaluating

Table 5. The real and imaginary parts of the first Fisher zeros for $u = \exp(-4\beta)$ (columns 4–5) versus lattice size L, evaluated from simulations at $\beta = \beta_{\mathrm{sim}} \approx \mathrm{Re}\, \beta^{(1)}$ (columns 2–3).

L	β_{sim}	$\mathrm{Re}\, \beta^{(1)}$	$\mathrm{Re}\, u^{(1)}$	$\mathrm{Im}\, u^{(1)}$
4	0.2327517	0.2327392(37)	0.3842870(59)	−0.0877415(55)
6	0.228982187	0.2289856(28)	0.3975550(44)	−0.0454038(44)
8	0.22674832	0.2267531(27)	0.4027150(44)	−0.0285905(42)
12	0.224558048	0.2245557(17)	0.4070191(28)	−0.0149314(25)
16	0.223560276	0.2235605(12)	0.4088085(19)	−0.0094349(17)
24	0.22268819	0.22268780(72)	0.4103176(12)	−0.0049422(11)
32	0.222317896	0.22231846(49)	0.41094218(81)	−0.00312478(84)
48	0.22200815	0.22200835(26)	0.41146087(43)	−0.00163982(49)
64	0.221880569	0.22188039(17)	0.41167349(29)	−0.00103825(37)
96	0.2217737	0.22177375(12)	0.41185008(21)	−0.00054521(19)
128	0.22173025	0.221730228(83)	0.41192200(14)	−0.00034552(14)
192	0.2216945	0.221694544(66)	0.41198091(11)	−0.00018140(11)
256	0.2216798	0.221679925(47)	0.412005022(77)	−0.000114660(82)
384	0.221668	0.221667926(38)	0.412024810(63)	−0.000060289(64)

Table 6. The real and imaginary parts of the second Fisher zeros for $u = \exp(-4\beta)$ (columns 4–5) versus lattice size L, evaluated from simulations at $\beta = \beta_{\rm sim} \approx \mathrm{Re}\,\beta^{(2)}$ (columns 2–3).

L	$\beta_{\rm sim}$	$\mathrm{Re}\,\beta^{(2)}$	$\mathrm{Re}\,u^{(2)}$	$\mathrm{Im}\,u^{(2)}$
4	0.2464072	0.246484(18)	0.344470(27)	−0.143307(23)
32	0.22313686	0.223169(15)	0.409529(25)	−0.004891(25)
64	0.222166355	0.2221781(85)	0.411182(14)	−0.001616(13)

$R = \langle\cos(\xi E)\rangle_\eta + i\langle\sin(\xi E)\rangle_\eta$ (where E is energy) by the histogram reweighting method and minimizing $|R|$ (see Ref. 11). Reliable results are ensured by the fact that, for each L, the simulation is performed at the coupling $\beta_{\rm sim}$ which is close to $\mathrm{Re}\,\beta^{(1)}$ — see Table 5. We have reached it by using the results of Ref. 11 and finite-size extrapolations. We have also estimated the second zeros for $L = 4, 32, 64$ from different simulation runs — see Table 6.

Our results in Tables 5 and 6 are reasonably consistent with those of Ref. 11, but are more accurate and include larger lattice sizes. Like in Ref. 11, the results for the second zeros are much less accurate than those for the first zeros.

4. Monte Carlo Analysis

4.1. *Estimation of the critical coupling*

Our results for $\tilde\beta_c(L)$ allow a very accurate estimation of the critical coupling β_c. The estimation from the data within $L \le 1536$ has been already considered in Ref. 12. In that paper, we have found it reasonable to discard the smallest sizes $L < 64$ and fit the data to the ansatz

$$\tilde\beta_c(L) = \beta_c + a_0 L^{-\frac{1}{\nu}} + a_1 L^{-\frac{1}{\nu}-\omega}, \tag{6}$$

with fixed exponents ν and ω. Here, we have performed a refined estimation, including the new values of $\tilde\beta_c(L)$ up to $L = 2560$ in Table 1. Using the widely accepted exponents $\nu = 0.63$ and $\omega = 0.832$, stated in Ref. 9, the fit within $L \in [64, 2560]$ gives $\beta_c = 0.2216546208(42)$. The χ^2 per degree of freedom of this fit is $\chi^2/\mathrm{d.o.f.} = 0.92$. There is some uncertainty concerning the values of ν and ω. Fortunately, the fit results are rather robust. In particular, using the exponents $\nu = 2/3$ and $\omega = 1/8$, considered in Refs. 6 and 7, we obtain $\beta_c = 0.2216546012(66)$ with $\chi^2/\mathrm{d.o.f.} = 0.89$. This estimate well compares with the most accurate values of β_c provided by other authors, i.e. $\beta_c = 0.22165455(5)$ (Ref. 21) and $\beta_c = 0.22165457(3)$.[22]

4.2. *Estimation of ω from MC data for very large lattice sizes $L \le 2560$*

The exponent ω describes corrections to the asymptotic finite-size scaling. In particular, for the susceptibility at $\beta = \tilde\beta_c(L)$ we have

$$\chi \propto L^{2-\eta}(1 + aL^{-\omega} + o(L^{-\omega})). \tag{7}$$

We define the effective exponent $\eta_{\rm eff}(L)$ as the mean slope of the $-\ln(\chi/L^2)$ versus $\ln L$ plot, evaluated by fitting the data within $[L/2, 2L]$. It behaves asymptotically as $\eta_{\rm eff}(L) = \eta + \mathcal{O}(L^{-\omega})$. It has been mentioned in Ref. 12 that ω might be as small as $1/8$, since the plot of the effective exponent $\eta_{\rm eff}$ versus $L^{-1/8}$ looks rather linear for large lattice sizes (see Fig. 6 in Ref. 12). This observation is confirmed also by the extended data here. The best linearity of $\eta_{\rm eff}(L)$ versus $L^{-\omega}$ plot within $L \in [96, 1280]$ (extracted from the susceptibility data within $L \in [48, 2560]$) is observed at $\omega = 0.16(36)$. This plot looks, indeed, much more linear at $\omega = 0.16$ than at $\omega = 0.8303$, as it can be seen from Fig. 1. The latter value comes from the estimate $\omega = 0.8303(18)$, obtained by the conformal bootstrap method in Ref. 23, which agrees with the MC value 0.832(6) of Ref. 9, but is claimed to be more accurate. Other MC values, usually reported in literature, are between 0.82 and 0.87 (see Refs. 8 and 9). The perturbative RG estimates are somewhat smaller, e.g. $\omega = 0.799 \pm 0.011$ (Ref. 3) and $\omega = 0.782(5)$.[24] The critical exponent $\eta = 0.03631(3)$, estimated in Ref. 23, is also indicated in Fig. 1 for comparison. The MC value of Ref. 9, $\eta = 0.03627(10)$, is very similar.

Although the conformal bootstrap method[23,25] gives apparently very accurate values of the critical exponents, it is based on a set of hypotheses, which are not rigorously and nonperturbatively proven. Therefore, we rely on MC simulations for large enough lattice sizes as the basic nonperturbative method of testing. The agreement between the predictions of the conformal bootstrap method[23] and the MC estimations of Ref. 9 is indeed convincing. However, our simulations for much larger lattice sizes ($L \leq 2560$ here versus $L \leq 360$ in Ref. 9), as well as our nonperturbative analytical arguments (theorem),[14] do not show such a perfect agreement.

An estimate of ω can be obtained by fitting the $\eta_{\rm eff}(L)$ data to the ansatz

$$\eta_{\rm eff}(L) = \eta + \mathcal{B}L^{-\omega}. \tag{8}$$

We have used also a more direct method, which gives similar, but slightly more accurate results. We consider the ratio $\Phi_b(L) = b^{-4}\chi(bL)/\chi(L/b)$ at $\beta = \tilde{\beta}_c(L)$,

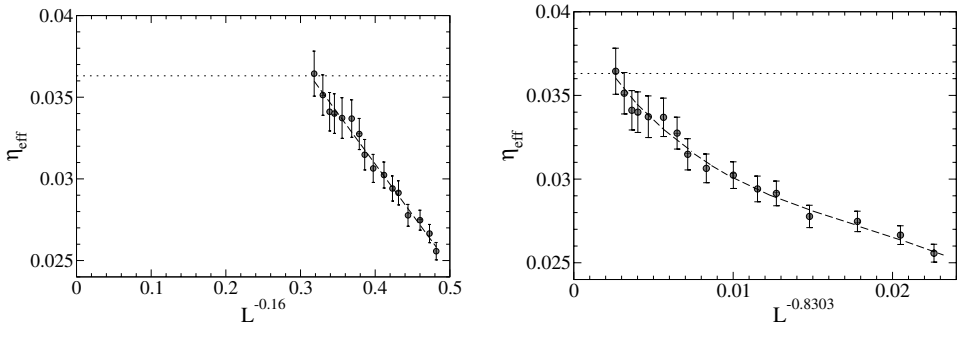

Fig. 1. The effective exponent $\eta_{\rm eff}(L)$ depending on $L^{-0.16}$ (left) and $L^{-0.8303}$ (right), evaluated from MC data at $\beta = \tilde{\beta}_c(L')$ with $L' \leq 2560$. The dashed straight lines represent the linear fit (left) and a guide to eye (right). One of the known estimates $\eta = 0.03631(3)$ (Ref. 23) is indicated by dotted lines.

where b is a constant. According to (7), $\Phi_b(L)$ behaves as

$$\Phi_b(L) = A + BL^{-\omega} \tag{9}$$

at $L \to \infty$, where $A = b^{-2\eta}$ and $B = ab^{-2\eta}(b^{-\omega} - b^{\omega})$. The correction amplitude B is larger for a larger b value, whereas a smaller b value allows us to obtain more data points for $\Phi_b(L)$. The actual choice $b = 2$ is found to be optimal for our data.

We have fit the effective exponent $\eta_{\text{eff}}(L)$ to (8) and the quantity $\Phi_2(L)$ to (9) within $L \in [L_{\min}, 1280]$ (estimated from the χ/L^2 data within $L \in [L_{\min}/2, 2560]$) to evaluate the correction-to-scaling exponent ω. The results are collected in Tables 7 and 8, respectively. The estimated ω values are essentially decreased for $L_{\min} \geq 80$ as compared to smaller $L_{\min}$ values. Moreover, the quality of fits is remarkably improved in this case, i.e. the values of χ^2/d.o.f. become smaller.

The value $\omega = 0.16(36)$ at $L_{\min} = 96$ in Table 7 is used in Fig. 1. It is not fully consistent with the usually accepted values of about 0.83. However, it is consistent with the relation $\omega \leq \omega_{\max} \approx 0.38$ stated at the end of Sec. 2, following from the theorem in Ref. 14. Similarly, the values 0.21(29) at $L_{\min} = 80$ and 0.04(33) at $L_{\min} = 96$ in Table 8 do not fully agree with $\omega \approx 0.83$, but are consistent with $\omega \leq \omega_{\max} \approx 0.38$. In fact, these estimates closely agree with the already mentioned value of $\omega = 1/8$, expected from the alternative theoretical treatment (GFD theory) of Ref. 6. In particular, the $\Phi_2(L)$ versus $L^{-1/8}$ plot is almost linear for large enough L, as shown in Fig. 2. Thus, ω could be as small as $1/8$.

Table 7. The correction-to-scaling exponent ω extracted from fits to (8) within $L \in [L_{\min}, 1280]$, using the MC data for $\chi(L')$ within $L' \in [24, 2560]$.

$L_{\min}$	ω	χ^2/d.o.f.
48	1.11(15)	1.34
54	1.04(19)	1.35
64	0.74(25)	0.89
80	0.39(32)	0.45
96	0.16(36)	0.21

Table 8. The correction-to-scaling exponent ω extracted from fits to (9) within $L \in [L_{\min}, 1280]$, using the MC data for $\chi(L')$ within $L' \in [24, 2560]$.

$L_{\min}$	ω	χ^2/d.o.f.
48	0.93(15)	1.19
54	0.94(20)	1.26
64	0.68(26)	1.13
80	0.21(29)	0.71
96	0.04(33)	0.69

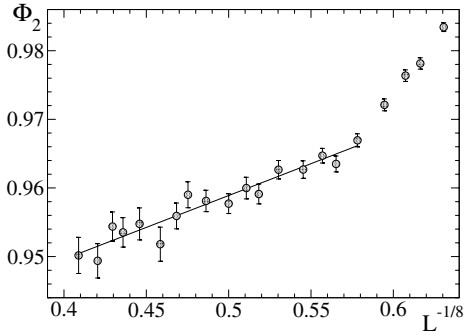

Fig. 2. The ratio $\Phi_2(L) = \chi(2L)/\chi(L/2)$, evaluated from MC data at $\beta = \tilde{\beta}_c(L)$, depending on $L^{-1/8}$. The straight line is the linear fit within $L \in [80, 1280]$.

The large statistical errors of our MC estimations still do not allow to make final conclusions. In particular, the observed deviations from the usual ω value of ≈ 0.83 are not much larger than 2σ, where σ is the standard deviation. One could argue that these deviations are caused by somewhat larger than usual statistical fluctuations in the data. The values of χ^2/d.o.f. of the fits provide an important extra criterion. Note that χ^2/d.o.f. is about unity for moderately good fits, and smaller χ^2/d.o.f. means better fit.[26] Relatively small χ^2/d.o.f. values can be expected for the fits of our $\eta_{\text{eff}}(L)$ data, since these data are obtained by fitting the original susceptibility values over strongly overlapping intervals. However, at least for the $\Phi_2(L)$ fits, χ^2/d.o.f. > 1 would be expected for unusually large fluctuations (frequently exceeding 2σ) in the susceptibility data. Thus, the small values of χ^2/d.o.f. at $L_{\min} \geq 80$ in Table 8 show the absence of such large fluctuations, implying that our MC estimation is reliable in this aspect. Hence, with a large probability, ω is, indeed, remarkably smaller than 0.83.

Our estimates $\omega = 0.16(36)$, $\omega = 0.21(29)$ and $\omega = 0.04(33)$ formally allow even negative values of ω within the statistical error bars. This, however, is not a real problem. Indeed, ω estimated from a fit to $A + BL^{-\omega}$ over $L \in [L_{\min}, L_{\max}]$, gives an effective exponent $\omega_{\text{eff}}(L_{\min}, L_{\max})$, which can be either positive or negative. The only requirement is that ω_{eff} must converge to a positive asymptotic value for $L_{\min}$ and $L_{\max}$ tending to infinity. In principle, ω_{eff} can decrease from positive to negative values and then converge to a positive asymptotic value. The estimation remains stable when ω_{eff} changes the sign.

For example, estimating ω_{eff} from Φ_2 values at L/c, L and cL with some constant $c > 1$, we obtain

$$\omega_{\text{eff}}(L) = -\frac{1}{\ln c} \times \ln\left[\frac{\Phi_2(cL) - \Phi_2(L)}{\Phi_2(L) - \Phi_2(L/c)}\right]. \tag{10}$$

Hence, $\omega_{\text{eff}}(L)$ is varied continuously with the values of $\Phi_2(L/c)$, $\Phi_2(L)$ and $\Phi_2(cL)$ in the vicinity of $\omega_{\text{eff}}(L) = 0$. In fact, the logarithmic behavior $\Phi_2(L) = A' + B' \ln L$

gives $\omega_{\rm eff} = 0$, and the fit ansatz $\Phi_2(L) = A + BL^{-\omega}$ at $\omega \to 0$ is consistent with the known representation $\ln L = \lim_{\Delta\to 0}[(L^{\Delta} - 1)/\Delta]$, where $\Delta = -\omega$.

Of course, if we use $\omega_{\rm eff}$ as an approximation for the true ω, then we must take into account the fact that $\omega > 0$. For example, from the MC estimate $\omega = 0.21(29)$ we can conclude that ω, most probably, lies in the interval $0 < \omega < 0.5$.

4.3. *Different estimations of ω from MC data for relatively small lattice sizes $L \leq 384$*

The known MC estimations of critical exponents by other authors are based on much smaller lattice sizes than in our studies. In particular, the data for $L \leq 360$ have been used in Ref. 9 for the estimation of ω, and even smaller lattice sizes are typically considered in other papers. Here we have performed a systematic study to compare results, provided by different methods of estimation of ω from finite-size scaling, using the same intervals of sizes $L \in [L_{\rm min}, 384]$. In this case, the maximal size $L = 384$ is similar to $L = 360$ in Ref. 9, but is much smaller than $L = 2560$ in Sec. 4.2.

We have denoted by ω_i the value of ω obtained by fitting the quantity Q_i to the ansatz

$$Q_i = A_i + B_i L^{-\omega}, \tag{11}$$

where $i = 1, 2, 3, 4$. The quantity $Q_1 = {\rm Im}\, u/(|u - u_c|)$ is determined from partition function zeros in Sec. 3.2, following the method of Ref. 11. Here u is the partition function zero in variable $u = \exp(-4\beta)$, u_c being its critical value $u_c = \exp(-4\beta_c)$. The approximate value 0.2216546 of critical coupling β_c has been used here, as in Ref. 11. It is fully consistent with the estimates, discussed at the end of Sec. 4.1. The quantities Q_2, Q_3 and Q_4 are the U values at pseudo-critical couplings $\grave{\beta}_c$, $\bar{\beta}_c$ and $\hat{\beta}_c$, corresponding to $Z_a/Z_p = 0.5425$, $\xi_{\rm 2nd}/L = 0.6431$ and maximum of specific heat, respectively, provided in Secs. 3.1.3–3.1.5. In addition, we have used also the quantity U_6 instead of U at pseudo-critical couplings $\grave{\beta}_c$ and $\bar{\beta}_c$, denoting the corresponding values of ω by ω_2' and ω_3'. The results at three values of the minimal lattice size, i.e. $L_{\rm min} = 8, 12, 16$, are collected in Table 9.

The corresponding values of χ^2/d.o.f., characterizing the quality of the fits, are listed in Table 10. One can judge from these values that $L_{\rm min} = 8$ is a good choice for the estimation of ω_2, ω_2' and ω_4, whereas $L_{\rm min} = 12$ is preferable in the remaining three cases.

Table 9. Estimates of the exponent ω, i.e. ω_1, ω_2, ω_2', ω_3, $\omega\prime_3$ and ω_4, obtained by fitting different quantities to the ansatz of the form (11) within $L \in [L_{\rm min}, 384]$ — see the text.

$L_{\rm min}$	ω_1	ω_2	ω_2'	ω_3	ω_3'	ω_4
8	0.758(16)	0.908(12)	0.911(12)	0.9027(84)	0.9031(75)	1.247(73)
12	0.880(32)	0.903(23)	0.913(22)	0.879(15)	0.879(13)	1.24(16)
16	0.902(48)	0.949(37)	0.945(32)	0.870(23)	0.866(21)	1.46(29)

Table 10. The values of χ^2/d.o.f., denoted as x_1, x_2, x_2', x_3, x_3' and x_4, corresponding to the fits for ω_1, ω_2, ω_2', ω_3, ω_3' and ω_4 at $L_{\min} = 8, 12, 16$ in Table 9.

$L_{\min}$	x_1	x_2	x_2'	x_3	x_3'	x_4
8	3.65	0.82	0.74	1.35	1.46	0.87
12	1.26	0.92	0.83	1.27	1.34	0.94
16	1.39	0.67	0.69	1.34	1.37	0.95

As we can see from Table 9, the results obtained from the scaling of U and U_6 always strongly correlate with each other. Moreover, the strong correlation between the values of U and U_6 can be seen from the data in Tables 3 and 4. From this point of view, there are only four essentially different methods considered, whereas the estimations of ω_2' and ω_3' should be considered as modifications of the methods for ω_2 and ω_3.

The estimates from partition function zeros (ω_1) are influenced by the assumed value of β_c. The influence, however, is quite insignificant for small variations in β_c within the error bars of the estimation in Sec. 4.1. In particular, the values of ω_1 in Table 9 are increased by $\approx 0.45\sigma$, if β_c is approximated by 0.22165462 instead of 0.2216546, in close agreement with one of the estimates in Sec. 4.1.

The cases of ω_3 and ω_3' represent the method used in Ref. 9. At $L_{\min} = 16$, our estimates of ω_3 and ω_3' agree marginally well with the result $\omega = 0.832(6)$ of Ref. 9, whereas generally the acceptable estimates in Table 9 (those with χ^2/d.o.f. < 1.5, skipping the most inaccurate value 1.46(29)) give larger values of ω, ranging from $\omega = 0.866(21)$ to $\omega = 1.247(73)$. Moreover, no convergence to the same value is seen, indicating that the lattice sizes $L \leq 384$ are still too small for a reliable estimation of the asymptotic correction-to-scaling exponent ω.

4.4. *Estimation of ω from the extended data for $\xi_{2\mathrm{nd}}/L = 0.6431$*

Apparently, the estimates of ω in Table 9 are larger than any of the known theoretical values. Therefore, a convergence to smaller value is expected for larger lattice sizes. We have tested such a possibility, using the data for U and U_6 at $\beta = \bar{\beta}_c(L)$ up to $L = 1536$ in Table 4. We have estimated the effective exponent $\omega_{\mathrm{eff}}(L)$ by fitting the $U(L')$ data and the $U_6(L')$ data to $A + BL'^{-\omega}$ within $L' \in [L, 32L]$. The obtained plots of $\omega_{\mathrm{eff}}(L)$ in these two cases are shown in Fig. 3.

An almost linear behavior of $\omega_{\mathrm{eff}}(L)$ versus $L^{-\omega}$ is expected in the case when the variation of $\omega_{\mathrm{eff}}(L)$ is governed by the second-order correction $\propto L^{-2\omega}$ to $U(L)$ or $U_6(L)$. We have used the $L^{-0.832}$ scale in Fig. 3 in accordance with $\omega = 0.832(6)$ reported in Ref. 9. The decrease of ω_{eff} with increase of L is, indeed, seen in Fig. 3. It shows that ω can be as small as $\omega = 0.832(6)$ (horizontal dashed lines) or even smaller.

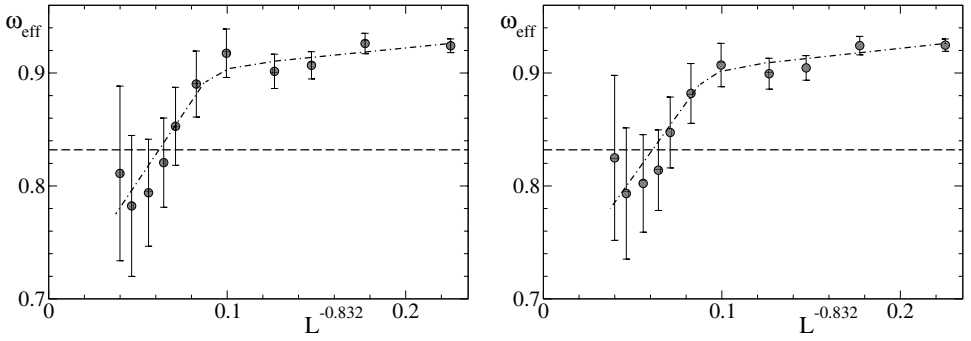

Fig. 3. The effective exponent $\omega_{\rm eff}(L)$, depending on $L^{-0.832}$, obtained by fitting the $U(L')$ data (left) and the $U_6(L')$ data (right) at $\beta = \tilde{\beta}_c(L')$ (the data from Table 4) to the ansatz $A + BL'^{-\omega}$ within $L' \in [L, 32L]$. Here, 0.832 is the value of ω, obtained in Ref. 9, which is indicated by horizontal dashed line. The dot–dashed curves are guides to eye.

4.5. *Influence of ω on the estimation of critical exponents η and ν*

As it can be seen from Figs. 1 and 2, corrections to scaling are remarkable and well detectable in our susceptibility data $\chi(L)$ at $\tilde{\beta}_c(L)$ (see Sec. 3.1.2). Indeed, the cases of $\eta_{\rm eff}(L) = \text{const.}$ and $\Phi_2(L) = \text{const.}$ correspond to the scaling without corrections, whereas Figs. 1 and 2 show certain variations. Moreover, according to our results, the correction-to-scaling exponent ω can be much smaller than the usually expected values of about 0.83. It can remarkably influence the estimation of the critical exponent η from the susceptibility data.

We have tested this effect by comparing η values, provided by fits of $\chi(L)$ to the expressions

$$\chi(L) = AL^{2-\eta}, \tag{12}$$

$$\chi(L) = AL^{2-\eta}(1 + bL^{-\omega}). \tag{13}$$

Equation (12) represents the ansatz without corrections to scaling. The corresponding values of η are further denoted by η_1. Equation (13) includes the leading correction to scaling, where the exponent ω has been fixed. We have considered three values of ω: 0.83, 0.38 and $1/8 = 0.125$. The first one is an approximate of the usual value, the second one is an approximate value of the upper bound $(\gamma - 1)/\nu$ considered in Sec. 2, and the third one is the already mentioned value of the GFD theory. We have denoted the corresponding estimates of η from (13) by η_2, η_3 and η_4, respectively. If ω is as small as $1/8$, then the second-order correction $\propto L^{-2\omega}$ and even higher order corrections can be very important. Therefore, we have tested also the ansatz

$$\chi(L) = AL^{2-\eta}(1 + b_1 L^{-1/8} + b_2 L^{-1/4}). \tag{14}$$

The corresponding values of η are denoted by η_5.

Table 11. Estimates of the exponent η depending on the fit interval $L \in [L_{\min}, 2560]$, using the ansatz (12) (estimate η_1), ansatz (13) with $\omega = 0.83$ (estimate η_2), $\omega = 0.38$ (estimate η_3) and $\omega = 0.125$ (estimate η_4), as well as the ansatz (14) (estimate η_5).

$L_{\min}$	η_1	η_2	η_3	η_4	η_5
16	0.02010(11)	0.03676(26)	0.05027(43)	0.08201(71)	0.02485(69)
32	0.02757(16)	0.03602(41)	0.04388(74)	0.0653(14)	0.0107(16)
64	0.03075(24)	0.03576(69)	0.0411(11)	0.0568(28)	0.077(26)

The results for η_i with $i = 1, 2, 3, 4, 5$, extracted from the fits within $L \in [L_{\min}, 2560]$ at $L_{\min} = 16, 32$ and 64 are collected in Table 11. The values of χ^2/d.o.f. of the corresponding fits are listed in Table 12. These values (x_1) are even much larger than unity for the fits without corrections to scaling. It implies that corrections to scaling are really important, and such fits are not acceptable. Concerning other fits, $L_{\min} = 32$ is well acceptable (χ^2/d.o.f. is small enough) for the fit with $\omega = 0.83$, and $L_{\min} = 64$ is well acceptable for the remaining fits with smaller ω values. Hence, the best estimates from (13) among those given in Table 11 are $\eta = 0.03602(41)$, $\eta = 0.0411(13)$ and $\eta = 0.0568(28)$ at $\omega = 0.83$, $\omega = 0.38$ and $\omega = 0.125$, respectively.

Thus, it turns out that our estimate of η agrees with the result of Ref. 9, i.e. $\eta = 0.03627(10)$, if the used value of ω is similar to that one in Ref. 9. However, smaller ω values lead to significantly larger estimates of η (i.e. 0.0411(13) and 0.0568(28)), so that the influence of ω is evident. Moreover, the best fit with two corrections to scaling at $\omega = 1/8$ (estimate η_5) suggests that η can have even larger value 0.077(26) if ω is, indeed, so small. The possibility that η is larger than ≈ 0.0363 is supported by any reasonable extrapolation of the effective exponent in Fig. 1, where this value is indicated by dotted lines.

We have performed similar tests also for the exponent ν, estimated from the $\partial Q/\partial\beta$ data at $\beta = \tilde{\beta}_c(L)$, considered in Sec. 3.1.2. In this case, the data can be reasonably well fit within $L \in [16, 2560]$ to the ansatz $\partial Q/\partial\beta = AL^{1/\nu}$ without corrections to scaling. The result is $1/\nu = 1.58754(37)$ or $\nu = 0.62991(15)$ with χ^2/d.o.f. $= 0.93$, in agreement with the value $\nu = 0.63002(10)$ of Ref. 9. Moreover, inclusion of the leading correction to scaling does not essentially change this result even for $\omega = 1/8$. Thus, there are almost no evidences that corrections to scaling are

Table 12. The values of χ^2/d.o.f., denoted as x_1, x_2, x_3, x_4 and x_5, corresponding to the fits for η_1, η_2, η_3, η_4 and η_5 at $L_{\min} = 16, 32, 64$ in Table 11.

$L_{\min}$	x_1	x_2	x_3	x_4	x_5
16	179	1.22	6.50	12.0	8.22
32	21.3	0.93	1.33	1.83	1.44
64	3.97	1.01	0.83	0.77	0.79

important in this case, except the fact that a very good fit within $L \in [64, 2560]$ to the ansatz $\partial Q/\partial\beta = AL^{1/\nu}(1 + b_1 L^{-1/8} + b_2 L^{-1/4})$ yields $1/\nu = 1.509(49)$ with $\chi^2/\text{d.o.f.} = 0.58$. It agrees with $\nu = 2/3$ predicted in Ref. 6.

A question can arise about the influence of ω value on the estimation of critical exponents in the case of improved Hamiltonians.[9,10] It is expected that the leading corrections to scaling vanish in this case, and therefore the influence of ω is small. However, in the case when the asymptotic corrections to scaling are described by the exponent $\omega \leq \omega_{\max} \approx 0.38$, as it is strongly suggested by the theorem discussed in Sec. 2, the vanishing of leading corrections cannot be supported by the existing MC analyses of such models. Indeed, in these analyses the asymptotic corrections to scaling are not correctly identified (probably, because of too small lattice sizes) if $\omega \leq \omega_{\max} \approx 0.38$, since one finds that $\omega \approx 0.8$.

5. Conclusions and Final Remarks

Nonperturbative analytical and MC arguments are provided in this paper, showing that corrections to scaling in the 3D Ising model are described by a remarkably smaller exponent ω than the usually accepted values of about 0.8 or 0.83. The analytical arguments in Sec. 2, which are based on the theorem proven in Ref. 14, suggest that $\omega \leq (\gamma - 1)/\nu$ holds, implying that ω cannot be larger than $\omega_{\max} = (\gamma - 1)/\nu \approx 0.38$ in the 3D Ising model. The analytical prediction of the GFD theory[6,7] is $\omega = 1/8$ in this case.

We have performed extensive MC simulations of the 3D Ising model (Sec. 3), including simulations on unusually large lattices, up to $L = 2560$, in order to test whether these challenging predictions can be confirmed by MC analysis of these data (Sec. 4). These predictions are supported by the estimation of ω from the susceptibility data up to $L = 2560$, discussed in Sec. 4.2. In particular, one of the estimates is $\omega = 0.21(29)$, implying that ω value, most probably, lies in the interval $0 < \omega < 0.5$.

The known MC estimates of ω, usually reported in literature, do not support our claim. In particular, the estimate $\omega = 0.832(6)$ has been reported in Ref. 9, citing also other results for ω value, typically ranging from 0.82 to 0.87. However, all these known MC estimates have been extracted from the data for relatively small (as compared to our $L = 2560$) lattice sizes, not exceeding $L = 360$. To verify whether such estimations objectively provide results always consistent with $\omega = 0.832(6)$ within the error bars (as one can judge from the review in Ref. 9), we have tested and compared the results of different known methods in a systematic way, i.e. by fitting the data within the same intervals $L \in [L_{\min}, 384]$ with $L_{\min} = 8, 12, 16$ (Sec. 4.3). Such $L_{\min}$ values are typical in many studies. Our tests include the known methods of estimation from partition function zeros, as well as from the scaling of $U = \langle m^4\rangle/\langle m^2\rangle^2$ and $U_6 = \langle m^6\rangle/\langle m^2\rangle^3$ at appropriate pseudo-critical couplings, corresponding to certain values of Z_a/Z_p and $\xi_{2\text{nd}}/L$. Our results in Table 9 have not confirmed an expectation that all such methods will give consistent results.

We conclude that the considered, in Sec. 4.3, sizes $L \leq 384$ are still too small for a reliable estimation of ω, since no convergence to the same asymptotic value is observed. The acceptable estimates in Table 9 (those with $\chi^2/\text{d.o.f.} < 1.5$, skipping the most inaccurate value 1.46(29)) range from $\omega = 0.866(21)$ to $\omega = 1.247(73)$ and, thus, are somewhat larger than any of the known theoretical values. Therefore, a convergence to smaller values is expected for larger lattice sizes. It has been confirmed by the analysis of the U and U_6 data within $L \leq 1536$ in the case of $\xi_{2\text{nd}}/L = 0.6431$ (Sec. 4.4). Namely, we conclude from Fig. 3 that ω can be as small as the value 0.832(6) of Ref. 9 (also obtained from the data for $\xi_{2\text{nd}}/L = 0.6431$) or even smaller.

We have tested how the estimation of the critical exponents η and ν is influenced by the choice of ω (Sec. 4.5). These tests have shown that the estimates of η, extracted from our susceptibility data for $L \leq 2560$, remarkably increase above the currently accepted values of about 0.036 for small ω. For example, from (13) we obtain $\eta = 0.0411(11)$ at $\omega = 0.38$ and $\eta = 0.0568(28)$ at $\omega = 0.125$. The influence on the estimation of ν is less evident.

As discussed in Ref. 14, our analytical predictions generally refer to a subset of n-vector models, where spin is an n-component vector with $n = 1$ in two dimensions and $n \geq 1$ in three dimensions. The MC analysis in Ref. 14 convincingly confirms these predictions for the scalar ($n = 1$) 2D φ^4 model. The 3D case with $n = 2$ has been tested in Ref. 7, based on accurate experimental data for specific heat in zero gravity conditions very close to the λ-transition point in liquid helium. The test in Sec. 4 of Ref. 7 reveals some inconsistency of the data with corrections to scaling proposed by the perturbative RG treatments, indicating that these corrections decay slower, i.e. $\theta = \nu\omega$ is smaller than usually expected. This finding is consistent with the theorem discussed in Sec. 2.

The mentioned here facts emphasize the importance of nonperturbative methods in a rigorous verification of results, proposed by perturbative treatments in the field of critical phenomena. In this respect, it is important to notice the recent work by Castellana and Parisi,[15] where it has been clearly shown that the perturbative RG method (ε-expansion) not always gives correct predictions. The results of Ref. 15 refer to the phase transitions in spin glasses, whereas our analytical and MC arguments allow us to question the validity and/or accuracy of the perturbative treatments even in the apparently very well studied case of the 3D Ising model.

It appears that there is some contradiction between the previous numerical results, including numerous MC estimations, and our actual findings. This apparent contradiction could be eventually resolved, relating the previous numerical results to a "perturbative" region, whereas our findings – to a "nonperturbative" region, as explained further on.

As it has been pointed out in (Sec. 5.4.6 of Ref. 27), it is, very likely, true that the ε-expansion at the critical point describes the behavior of correlation function(s) in the limit of $4 - d = \varepsilon \to 0$ for any fixed nonzero wave vector magnitude k, rather than the behavior at $k \to 0$ at a fixed small and positive ε. It implies that the predictions of the ε-expansion refer to an interval $k > k_{\min}(\varepsilon)$, where $k_{\min}(\varepsilon) \to 0$ at

$\varepsilon \to 0$. We propose that $k_{\min}(\varepsilon)$ is finite, but still very small at $\varepsilon = 1$. It explains the success of the ε-expansion and other, similar in essence, perturbative RG methods in reaching agreement with numerical results. Indeed, power-law singularities within $k < k_{\min}(\varepsilon)$ are irrelevant (smoothened) for an easily accessible by various numerical methods "perturbative" region of not too small reduced temperatures in the thermodynamic limit and not too large lattice sizes in the finite-size scaling regime. It explains the fact that these numerical methods easily produce results, which are approximately consistent with the estimates of the perturbative RG method and, therefore, also with each other. To the contrary, our findings refer to the "nonperturbative" asymptotic region, where relevant power-law singularities show up within $k < k_{\min}(\varepsilon)$. It corresponds to unusually large lattice sizes in the finite-size scaling regime and extremely small reduced temperatures in the thermodynamic limit. This is the region, which cannot be easily accessed and is not yet properly investigated by numerical methods.

From the perspective of the nonperturbative RG approach, the "nonperturbative" asymptotic region is described by certain nonperturbative fixed point. We assume that this fixed point is not described by the usual perturbative treatments to argue that the critical exponents can be inconsistent with the perturbative RG estimates. In fact, an evidence that such a nonperturbative fixed point can exist, which is not described in any way by the ε-expansion, has been provided in Ref. 15. In the case of spin glasses,[15] it describes the phase transition in the region of parameters of the Edwards–Anderson model, where no phase transition is predicted by the ε-expansion.

The results of the ε-expansion coincide very well with the Conformal Field Theory (CFT), considered in Refs. 23 and 25. This, however, only implies that the perturbative fixed point is, indeed, conformally symmetric and consistent with CFT at specific constraints, assumed in Refs. 23 and 25, to obtain the values of the critical exponents.

Acknowledgments

This work was made possible by the facilities of the Shared Hierarchical Academic Research Computing Network (SHARCNET:www.sharcnet.ca). The authors acknowledge the use of resources provided by the Latvian Grid Infrastructure and High Performance Computing centre of Riga Technical University. R. M. acknowledges the support from the NSERC and CRC program.

References

1. D. J. Amit, *Field Theory, the Renormalization Group, and Critical Phenomena* (World Scientific, Singapore, 1984).
2. S. K. Ma, *Modern Theory of Critical Phenomena* (W. A. Benjamin, New York, 1976).
3. J. Zinn-Justin, *Quantum Field Theory and Critical Phenomena* (Clarendon Press, Oxford, 1996).

4. H. Kleinert and V. Schulte-Frohlinde, *Critical Properties of ϕ^4 Theories* (World Scientific, Singapore, 2001).
5. A. Pelissetto and E. Vicari, *Phys. Rep.* **368**, 549 (2002).
6. J. Kaupužs, *Ann. Phys. (Berlin)* **10**, 299 (2001).
7. J. Kaupužs, *Canadian J. Phys.* **9**, 373 (2012).
8. M. Hasenbusch, *Int. J. Mod. Phys. C* **12**, 911 (2001).
9. M. Hasenbusch, *Phys. Rev. B* **82**, 174433 (2010).
10. M. Hasenbusch, *Phys. Rev. B* **82**, 174434 (2010).
11. A. Gordillo-Guerro, R. Kenna and J. J. Ruiz-Lorenzo, *J. Stat. Mech.* **2011**, P09019 (2011).
12. J. Kaupužs, J. Rimšāns and R. V. N. Melnik, *Ukr. J. Phys.* **56**, 845 (2011).
13. J. Kaupužs, R. V. N. Melnik and J. Rimšāns, *Commun. Comp. Phys.* **14**, 355 (2013).
14. J. Kaupužs, R. V. N. Melnik and J. Rimšāns, *Int. J. Mod. Phys. C* **27**, 1650108 (2016).
15. M. Castellana and G. Parisi, *Sci. Rep.* **5**, 12367 (2015).
16. U. Wolff, *Phys. Rev. Lett.* **62**, 361 (1989).
17. J. Kaupužs, J. Rimšāns and R. V. N. Melnik, *Phys. Rev. E* **81**, 026701 (2010).
18. M. Hasenbusch, *J. Phys. A: Math. Gen.* **32**, 4851 (1999).
19. M. Hasenbusch, *Int. J. Mod. Phys. C* **12**, 911 (2001).
20. M. Hasenbusch, private communication
21. Y. Deng and H. W. J. Blöte, *Phys. Rev. E* **68**, 036125 (2003).
22. J. A. Plascak, A. M. Ferrenberg and D. P. Landau, *Phys. Rev. E* **65**, 066702 (2002).
23. S. El-Showk, M. F. Paulos, D. Poland, S. Rychkov, D. Simmons-Duffin and A. Vichi, *J. Stat. Phys.* **157**, 869 (2014).
24. A. A. Pogorelov and I. M. Suslov, *J. Exp. Theor. Phys.* **106**, 1118 (2008).
25. F. Kos, D. Poland and D. Simmons-Duffin, *J. High Energy Phys.* **1406**, 091 (2014).
26. W. H. Press, B. P. Flannery, S. A. Teukolsky and W. T. Vetterling, *Numerical Recipes – The Art of Scientific Computing* (Cambridge University Press, Cambridge, 1989).
27. J. Kaupužs, *Int. J. Mod. Phys. A* **27**, 1250114 (2012).